Angewandte Chemie
Eine Zeitschrift der Gesellschaft Deutscher Chemiker

Supporting Information

Directed Evolution of a Halide Methyltransferase Enables Biocatalytic Synthesis of Diverse SAM Analogs

Qingyun Tang, Christoph W. Grathwol, Aşkın S. Aslan-Üzel, Shuke Wu, Andreas Link, Ioannis V. Pavlidis, Christoffel P. S. Badenhorst,* and Uwe T. Bornscheuer**

anie_202013871_sm_miscellaneous_information.pdf

Table of Contents

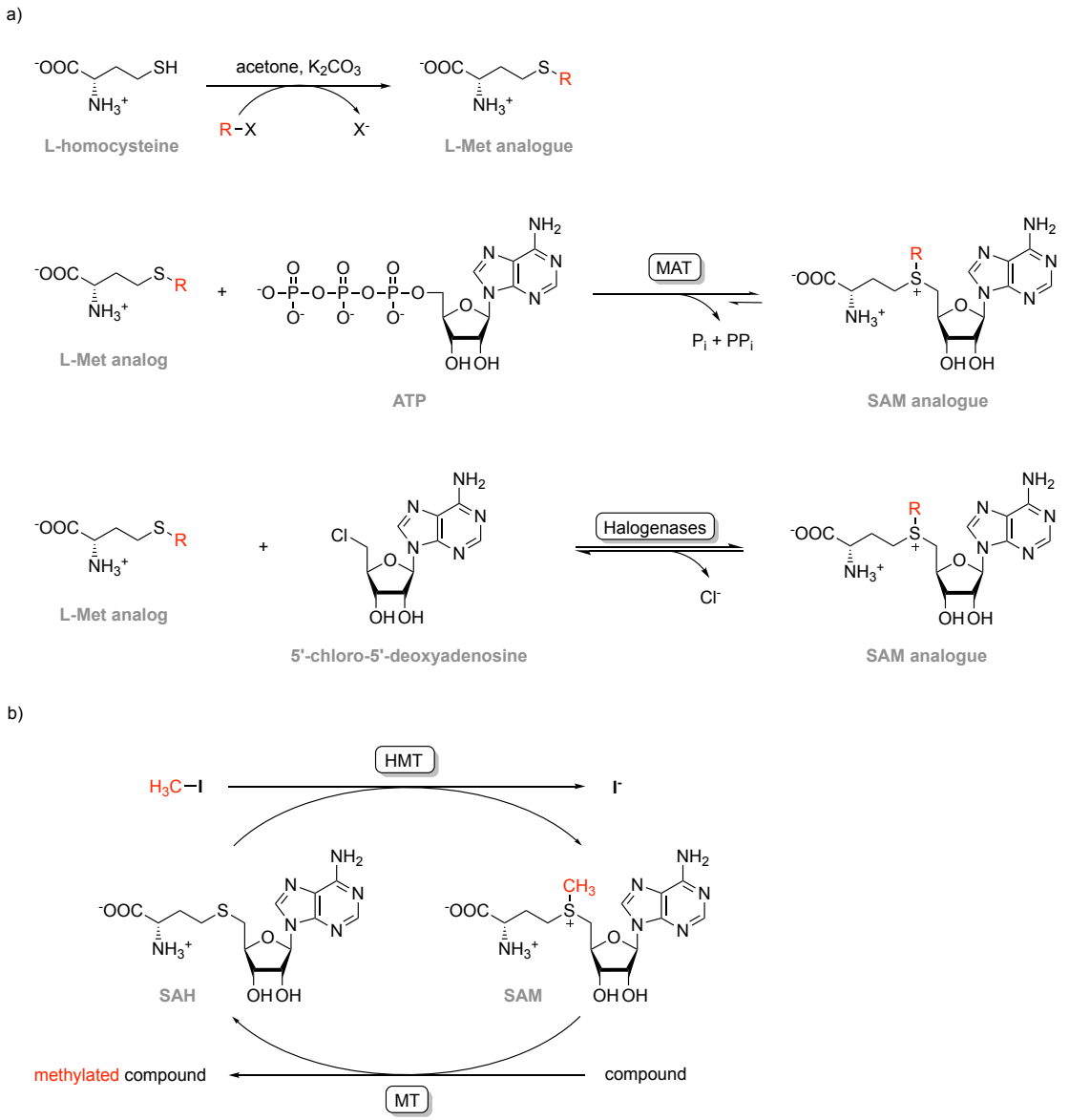

Figure S1. Enzymatic synthesis of SAM analogues. a) L-methionine analogues can be chemically synthesized from L-homocysteine and alkyl halides. Methionine adenosyltransferases (MATs) or halogenases can then use ATP or 5'-chloro-5'-deoxyadenosine, respectively, to convert the L-methionine analogues to the corresponding SAM analogues. **b)** Halide methyltransferases (HMTs) can convert *S*-adenosyl homocysteine (SAH) to *S*-adenosyl methionine (SAM) in a single step, using methyl iodide as alkyl donor. This enables a simple regeneration of SAM from SAH, facilitating methyltransferase (MT)-catalyzed methylation of acceptor compounds using only catalytic amounts of SAH.[1] The purpose of our study was to expand the substrate specificity of an HMT to allow SAM analogues to be synthesized.

Additional results

Initial characterization of different HMTs

Table S1. Specific activities (μmol/min/mg) of HMTs towards different alkyl iodides for synthesizing the corresponding SAM analogues.[a]

Enzyme				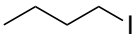
Arabidopsis thaliana HMT	5942 ± 204	2.69 ± 0.15	<0.01	<0.01
Chloracidobacterium thermophilum HMT	132 ± 9	0.11 ± 0.07	<0.01	<0.01
Raphanus sativus HMT	8457 ± 361	1.18 ± 0.11	<0.01	<0.01

[a] Reaction times were 10 min for methyl iodide and ethyl iodide, and 4h for propyl iodide and butyl iodide. Negative controls performed without enzyme were subtracted. Activities were determined using the iodide assay described in Figure S2 and Method S3. Data reported are the means and standard deviations calculated from three independent measurements.

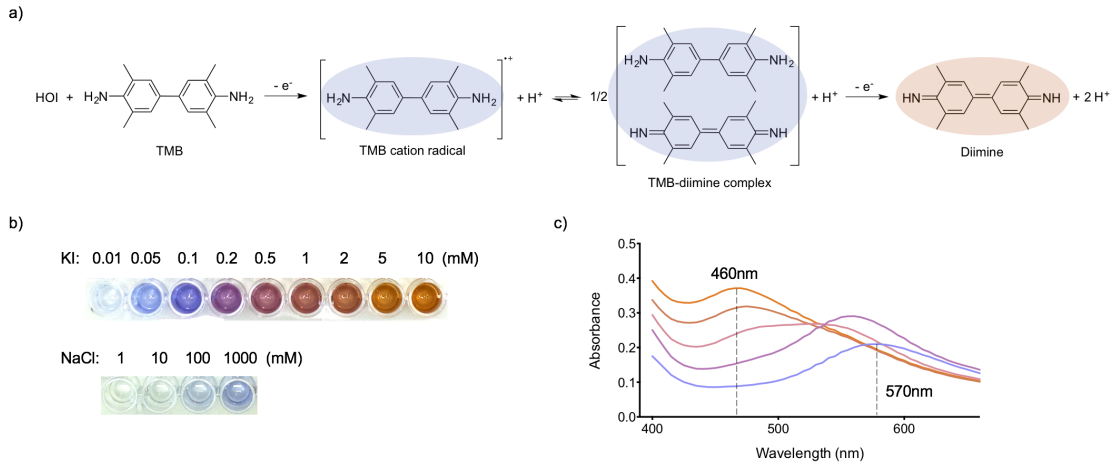

Figure S2. The iodide assay used for screening HMT libraries. a) Oxidation of TMB by HOI. **b)** Color of reaction mixtures of of KI and NaCl (1 µl; various concentrations) with the iodide assay solution (50 µl) after 30min. **c)** Absorbance spectra of the TMB oxidation products.

Comparison of the iodide assay to HPLC

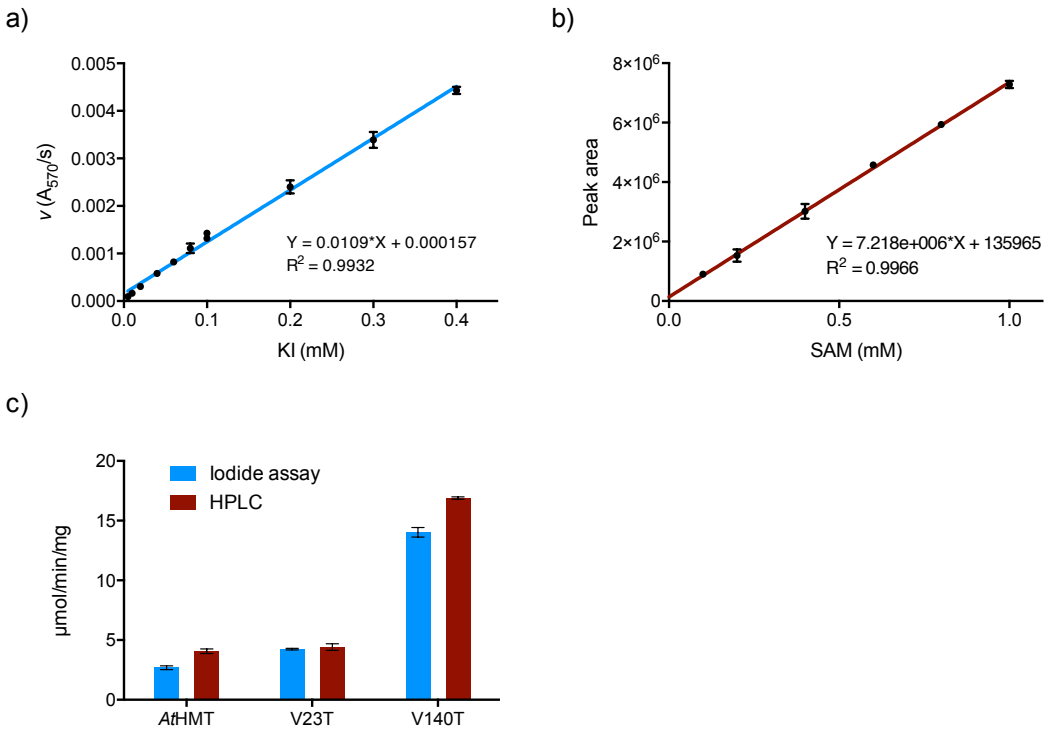

Figure S3. Comparison of the iodide assay to HPLC. a) Calibration curve for the iodide assay. The concentration of potassium iodide (KI) is plotted against the initial velocity of the increase in absorbance at 570 nm. **b)** Calibration curve for HPLC analysis of SAM. The concentration of SAM is plotted against the peak area determined by HPLC. **c)** Comparison of the ethyltransferase specific activities of wild-type *At*HMT and the V23T and V140T variants determined using the iodide assay and HPLC. Data plotted are the means and standard deviations calculated from three independent measurements.

Screening for improved ethyltransferase activity

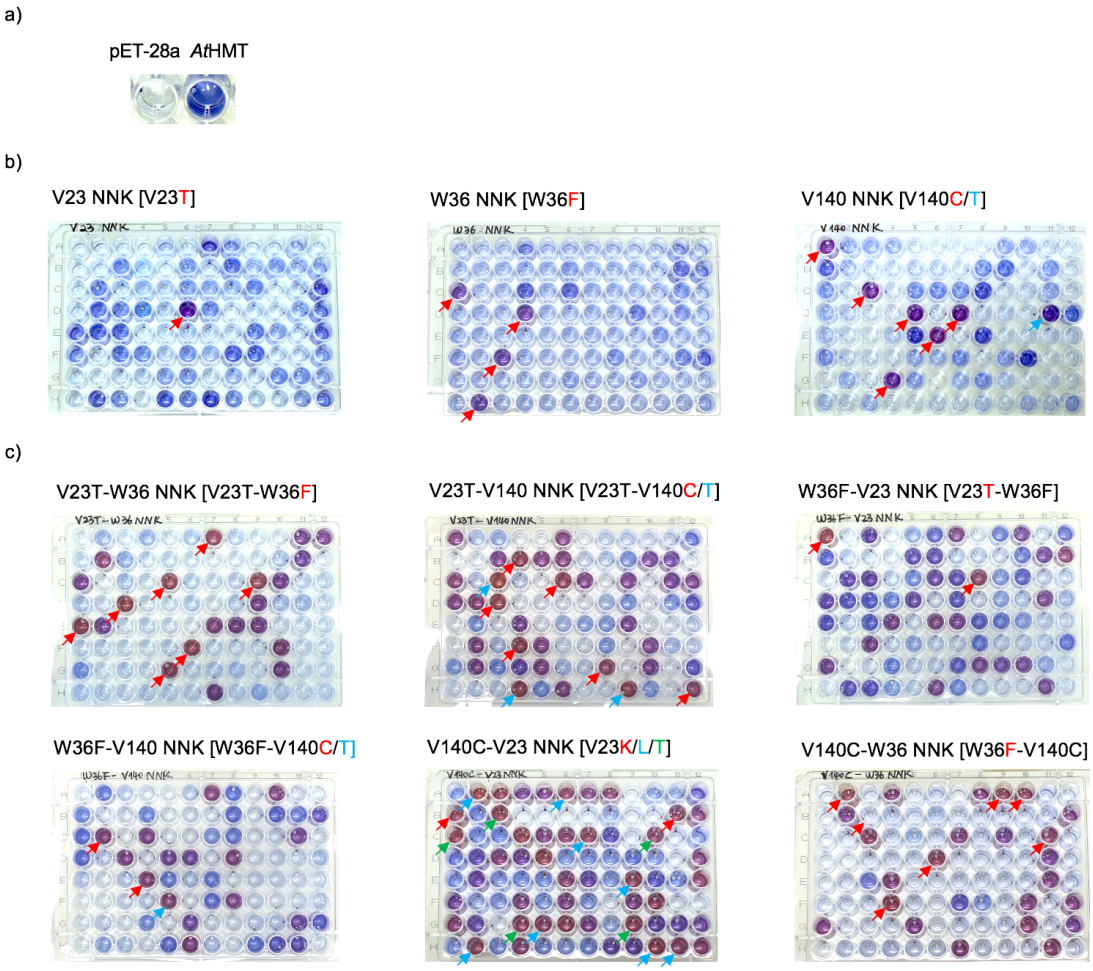

Figure S4. Examples of the iodide screening assay. Libraries were screened as described in Methods S2 and S3. **a)** The empty pET-28a vector and the wild-type *At*HMT as negative and positive controls, respectively. **b)** Screening of NNK libraries at positions V23, W36, and V140. Hits are indicated with colored arrows and named in square brackets. **c)** Screening of libraries at secondary positions. Hits are indicated with colored arrows and named in square brackets.

Table S2. Libraries screened and hits obtained.

Library	Hits
P20 NNK	-
V23 NNK	V23T
L27 NNK	-
W36 NNK	W36F
W47 NNK	-
Y139 NNK	-
V140 NNK	V140C/T
C143 NNK	-
Y172 NNK	-
R214 NNK	-
V23T-W36 NNK	V23T-W36F
V23T-V140 NNK	V23T-V140C/T
W36F-V23 NNK	V23T-W36F
W36F-V140 NNK	W36F-V140C/T
V140C-V23 NNK	V23K/L/T-V140C
V140C-W36 NNK	W36F-V140C

Characterization of the hits

Table S3. Specific activities (μmol/min/mg) of the wild-type *At*HMT and mutants against ethyl iodide for synthesizing SAE.

Enzyme variant	Specific activity[a]
*At*HMT	2.69 ± 0.15
V23T	4.24 ± 0.07
W36F	2.80 ± 0.35
V140C	9.74 ± 0.85
V140T	14.02 ± 0.40
V23T-W36F	3.81 ± 0.23
V23T-V140C	10.28 ± 0.94
V23T-V140T	8.77 ± 1.39
V23K-V140C	6.23 ± 0.34
V23L-V140C	9.00 ± 0.62
W36F-V140C	8.21 ± 0.73
W36F-V140T	1.95 ± 0.15
V23T-W36F-V140C	6.74 ± 0.11
V23K-W36F-V140C	0.42 ± 0.03
V23L-W36F-V140C	1.59 ± 0.27
V23T-W36F-V140T	1.32 ± 0.19

[a] Data reported are the means and standard deviations calculated from three independent measurements. The data are visualized in Figure 2 of the main paper.

Michaelis-Menten kinetics for methyltransferase activity

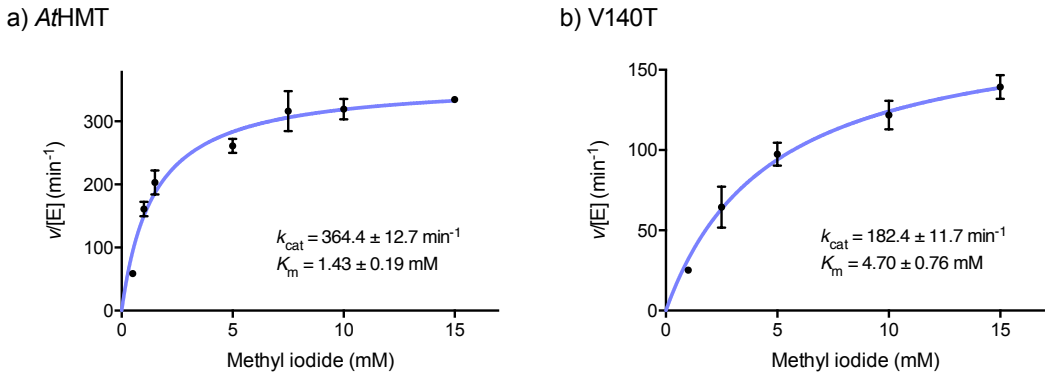

Figure S5. Michaelis-Menten kinetics for methyltransferase activity. a) Wild-type *At*HMT and **b)** the V140T variant. Activities at various methyl iodide concentrations were determined as described in Method S4.2. Data plotted are the means and standard deviations calculated from three independent measurements.

Michaelis-Menten kinetics for ethyltransferase activity

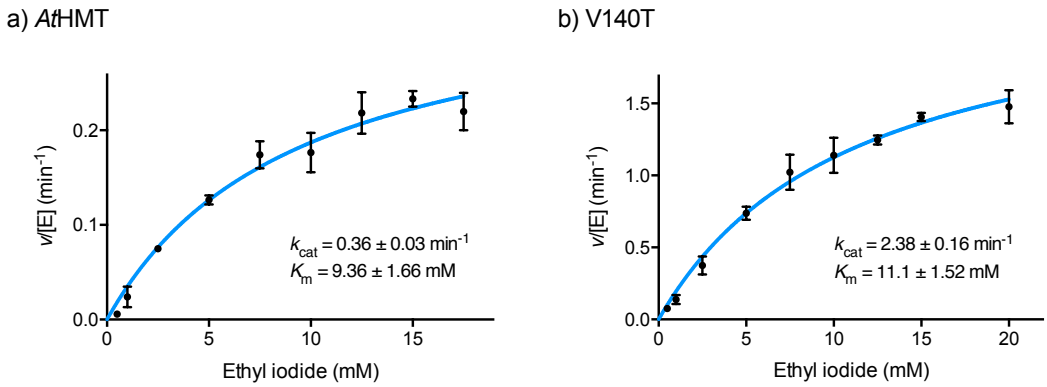

Figure S6. Michaelis-Menten kinetics for ethyltransferase activity. a) Wild-type *At*HMT and **b)** the V140T variant. Activities at various ethyl iodide concentrations were determined as described in Method S4.2. Data plotted are the means and standard deviations calculated from three independent measurements.

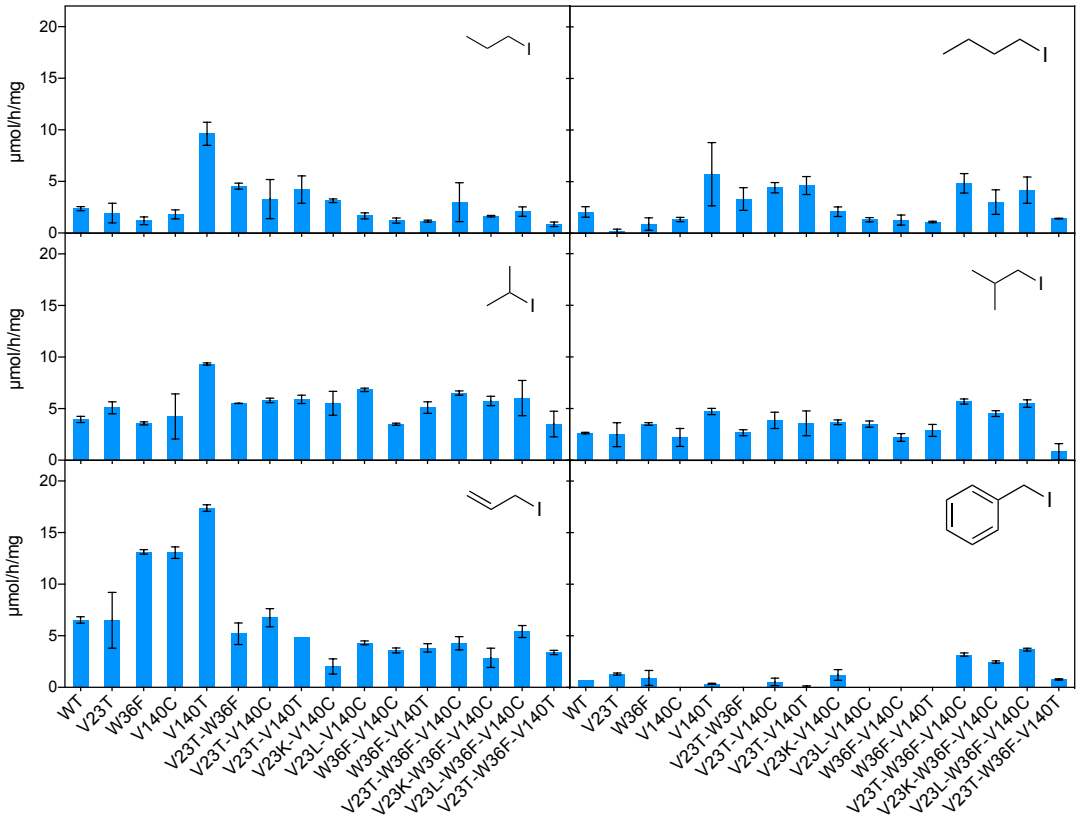

Figure S7. Specific activities (μmol/h/mg) of *At*HMT and several variants towards various alkyl iodides for synthesizing the corresponding SAM analogues. Specific activities were determined as described in Methods S3.3 and S4.2. Data plotted are the means and standard deviations calculated from two independent measurements.

Preparative scale synthesis of SAM analogues and product analysis

Table S4. Scaled-up production of SAM analogues.

SAH	Alkyl iodide	V140T *At*HMT	Product	Reaction time	Conversion[a]
15 mg (10 mM)	80 mM EtI	5.0 mg/ml (182 µM)	SAE (**2**)	14h	90%
15 mg (10 mM)	80 mM PrI	7.7 mg/ml (273 µM)	SAP (**3**)	24h	50%
15 mg (10 mM)	80 mM Allyl-I	5.0 mg/ml (182 µM)	SAA (**4**)	14h	70%

[a]Determined by HPLC (Figure S9).

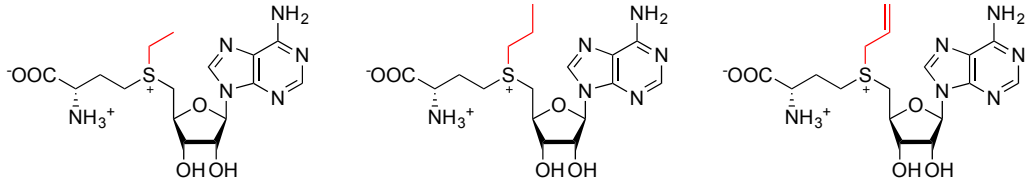

S-adenosyl L-ethionine (SAE), **2** *S*-propyl homocysteine (SAP), **3** *S*-allyl homocysteine (SAA), **4**

Figure S8. Structures of the SAM analogues. The iodoalkane-derived alkyl groups are shown in red.

a)

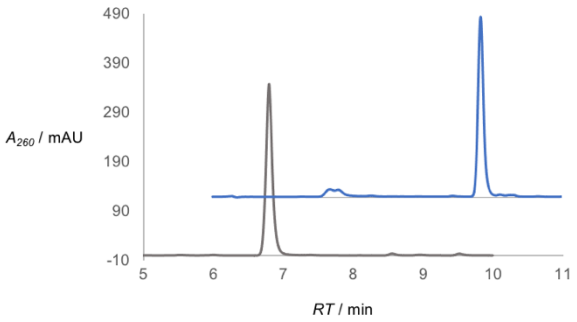

RT / min	Compound	- HMT		+ HMT	
		Area	%	Area	%
6.8	SAH	8,485,833	100	870,030	10
8.9	SAE	0	0	7,611,520	90

b)

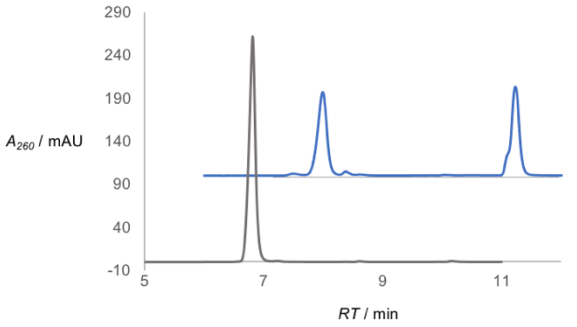

RT / min	Compound	- HMT		+ HMT	
		Area	%	Area	%
6.8	SAH	7,258,184	100	4,149,439	50
10.0	SAP	0	0	4,079,157	50

c)

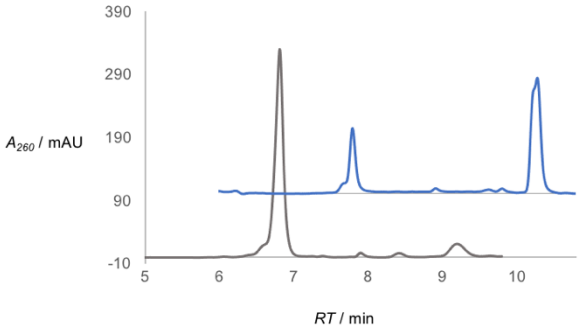

RT / min	Compound	- HMT		+ HMT	
		Area	%	Area	%
6.8	SAH	7,790,385	90.8	2,687,328	30
9.3	SAA	788,615	9.2	6,209,560	70

Figure S9. HPLC chromatograms of **a)** SAE (**2**), **b)** SAP (**3**), and **c)** SAA (**4**) syntheses on preparative scale. Structures of the SAM analogues are shown in Figure S8.

Preparative scale bioalkylation cascade reactions and product analysis

Table S5. Scaled-up production of alkylated products.

Substrate	Alkyl iodide	SAH	MT	HMT[a]	Product	Reaction time	Conversion [b]	Isolated yield	Number of cycles
5, 20 mg (10 mM)	EtI 80 mM	100 µM	IeOMT, 12 mg/ml (292 µM)	10 mg/ml (364 µM)	**6**	72h	41%	18%	41
7, 10 mg (10 mM)	PrI 80 mM	100 µM	COMT, 12 mg/ml (292 µM)	10 mg/ml (364 µM)	[c]	48h	5%	-	-
7, 10 mg (10 mM)	Allyl-I 80 mM	100 µM	COMT, 12 mg/ml (292 µM)	8 mg/ml (291 µM)	**8**	24h	48%	16%	48

[a] *At*HMT-V140T was used for all reactions. [b] Conversions were determined using HPLC (Figure S11). [c] Because of the low conversion, this product was not purified and identified by NMR spectroscopy.

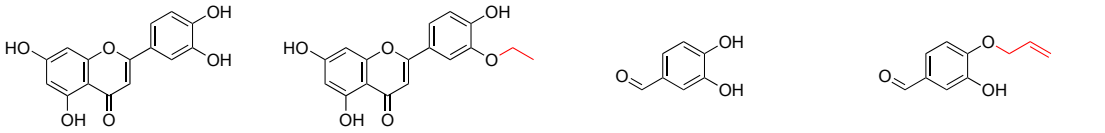

luteolin, **5** 3'-*O*-ethylluteolin, **6** 3,4-dihydroxybenzaldehyde, **7** 4-allyloxy-3-hydroxybenzaldehyde, **8**

Figure S10. Structures of substrates and alkylated products. The iodoalkane-derived alkyl groups are shown in red.

a)

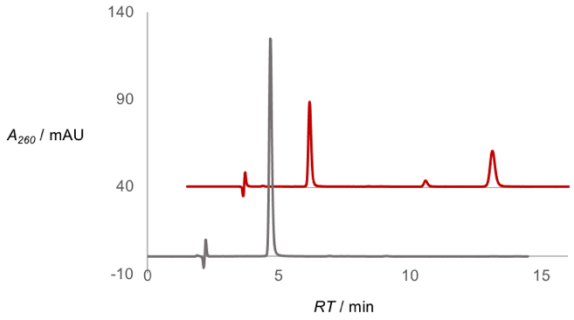

RT / min	Compound	- HMT/MT		+ HMT/MT	
		Area	%	Area	%
4.7	**5**	3,234,855	100	1,518,019	55
9.2	-	0	0	138,223	5
11.7	**6**	0	0	1,171,139	41

b)

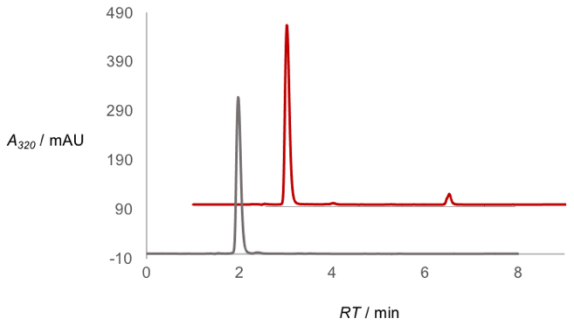

RT / min	Compound	- HMT/MT		+ HMT/MT	
		Area	%	Area	%
2.0	**7**	8,606,287	100	11,284,861	95
5.6	-	0	0	527,122	5

c)

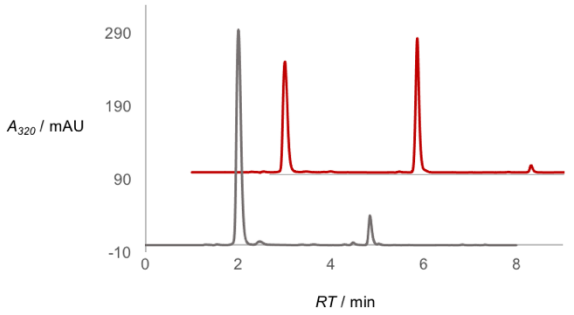

RT / min	Compound	- HMT/MT		+ HMT/MT	
		Area	%	Area	%
2.0	**7**	7,991,024	90.2	4,205,968	50
4.9	**8**	8,722,81	9.8	3,983,425	48
7.3	-	0	0	18,4431	2

Figure S11. HPLC chromatograms of **a)** luteolin (**5**) and the product 3′-*O*-ethylluteolin (**6**), **b)** 3,4-dihydroxylbenzaldehyde (**7**) and the propylated product, and **c)** 3,4-dihydroxylbenzaldehyde (**7**) and the product 4-allyloxy-3-hydroxy-benzaldehyde (**8**).

3′-*O*-ethylluteolin (6). ^{1}H NMR, H,H-COSY (400 MHz, DMSO-d_6): δ (ppm) = 12.96 (s, 1H, OH), 7.55 (d, J = 1.8 Hz, 1H, 6′-H), 7.53 (s, 1H, 2′-H), 6.94 (d, J = 8.9 Hz, 1H, 5′-H), 6.84 (s, 1H, 3-H), 6.47 (s, 1H, 8-H), 6.17 (s, 1H, 6-H), 4.15 (q, J = 7.0 Hz, 1H, 7′-H), 1.37 (t, J = 7.0 Hz, 1H, 8′-H); ^{13}C NMR, DEPT-135, HSQC, HMBC (101 MHz, DMSO-d_6): δ (ppm) = 181.7 (4), 165.1 (7), 163.6 (2), 161.4 (5), 157.4 (9), 151.2 (4′), 147.2 (3′), 121.4 (1′), 120.3 (6′), 115.9 (5′), 111.4 (2′), 103.4 (10), 103.1 (3), 99.0 (6), 94.2 (8), 64.2 (7′), 14.7 (8′).

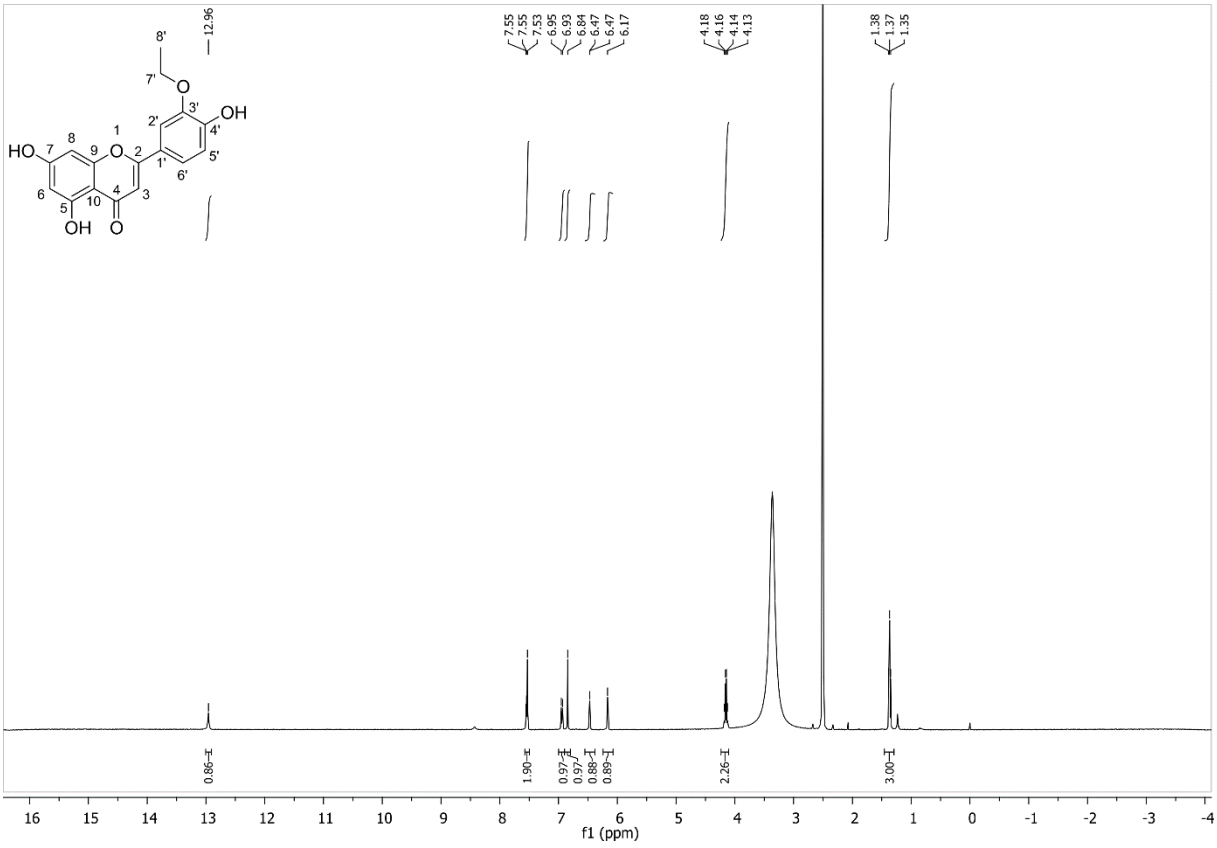

Figure S12. ^{1}H NMR spectrum of 3′-*O*-ethylluteolin (**6**).

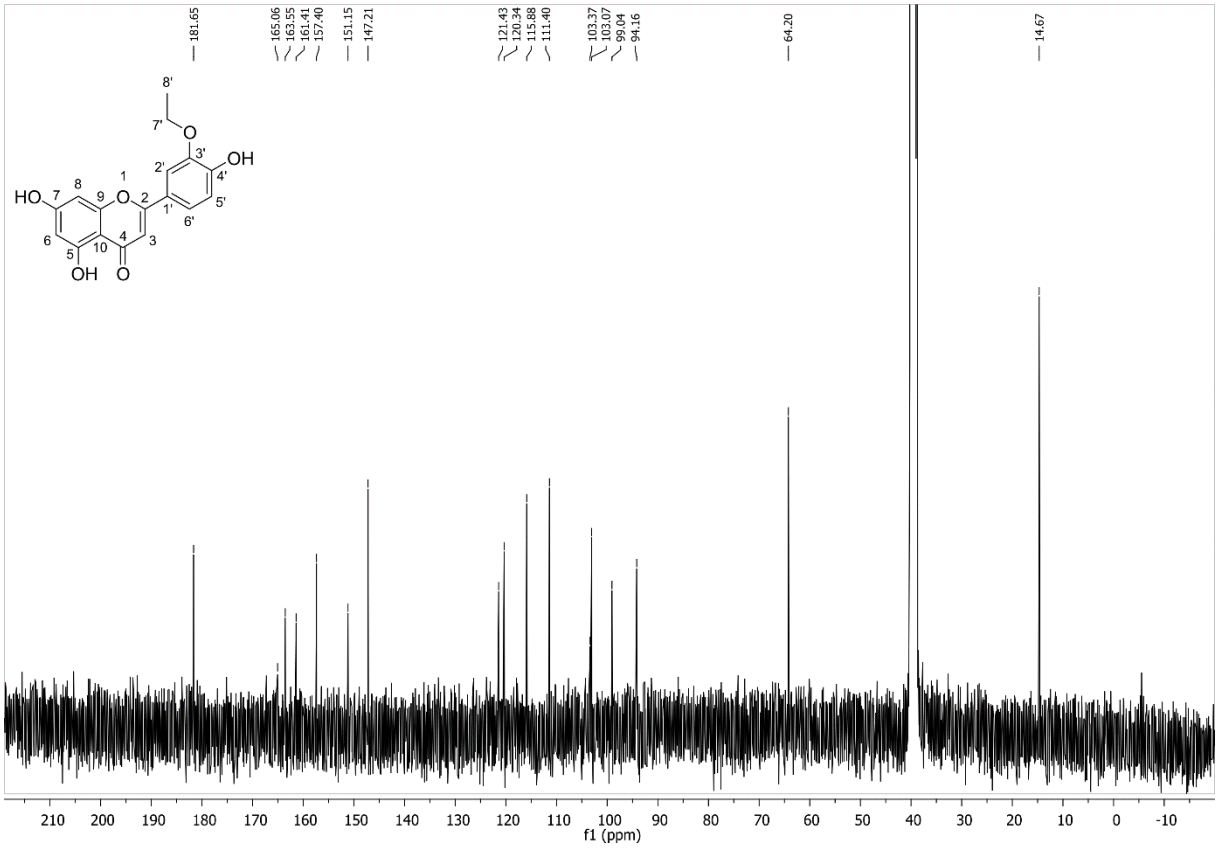

Figure S13. ^{13}C NMR spectrum of 3′-*O*-ethylluteolin (**6**).

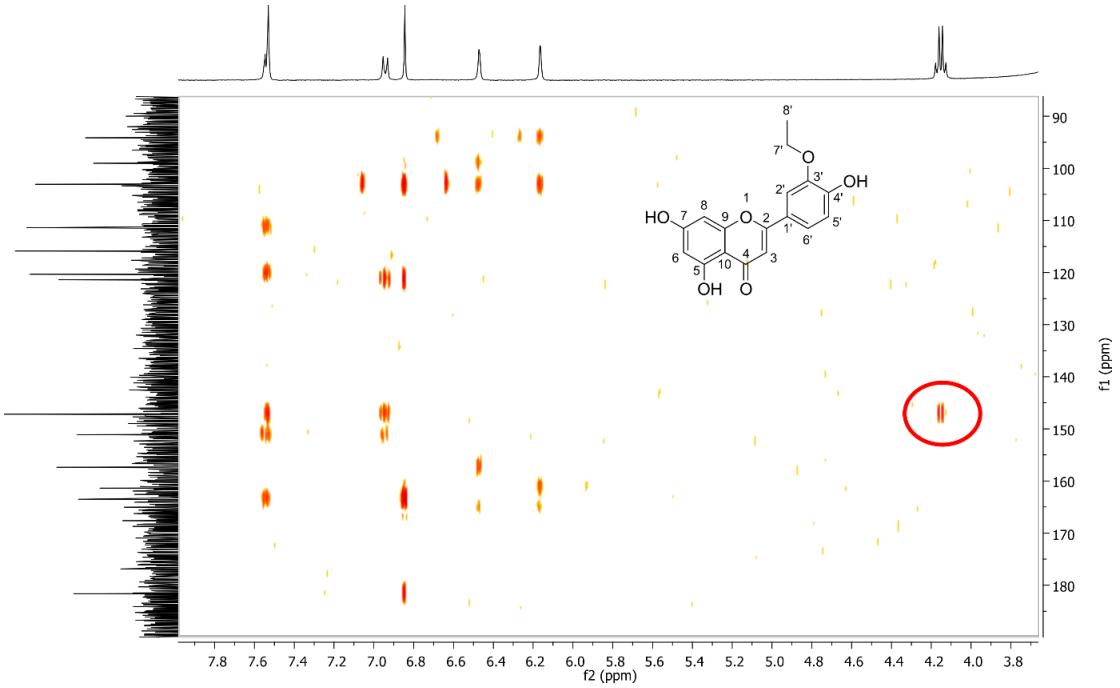

Figure S14. HMBC spectrum of 3′-*O*-ethylluteolin (**6**). The signal that defines the regioisomer is highlighted.

4-allyloxy-3-hydroxybenzaldehyde (8). ^{1}H NMR, H,H-COSY (400 MHz, DMSO-d_6): δ (ppm) = 9.77 (s, 1H, 7-H), 7.37 (dd, J = 8.3, 1.8 Hz, 1H, 6-H), 7.28 (d, J = 1.8 Hz, 1H, 2-H), 7.11 (d, J = 8.3 Hz, 1H, 5-H), 6.12–6.00 (m, 1H, 9-H), 5.44 (dd, J = 17.3, 1.6 Hz, 1H, 10-H_a), 5.29 (dd, J = 10.5, 1.5 Hz, 1H, 10-H_b), 4.68 (d, J = 5.2 Hz, 2H, 8-H); ^{13}C NMR, DEPT-135, HSQC, HMBC (101 MHz, DMSO-d_6): δ (ppm) =191.5 (7), 152.2 (4), 147.3 (3), 133.3 (9), 130.0 (1), 124.1 (6), 117.9 (10), 113.9 (2), 113.0 (5), 68.9 (8).

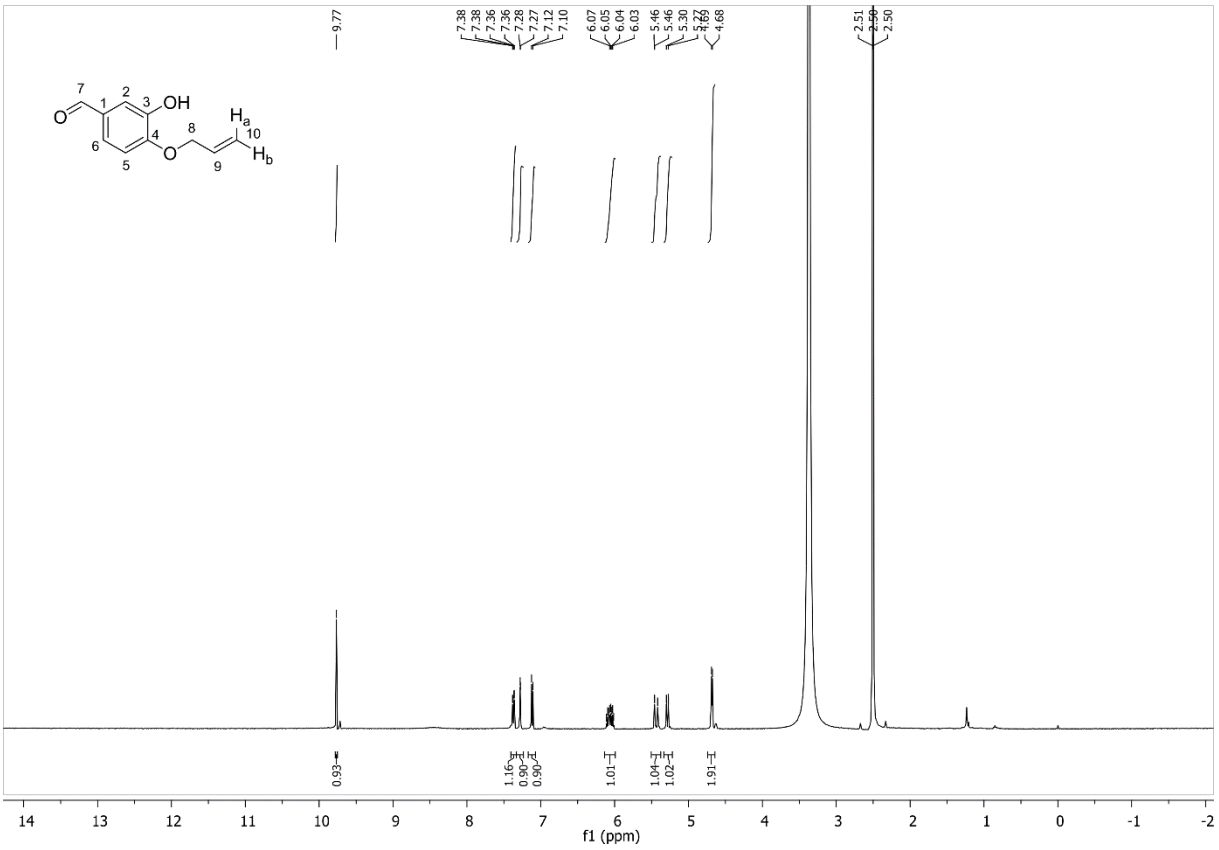

Figure S15. ^{1}H NMR spectrum of 4-allyloxy-3-hydroxybenzaldehyde (**8**).

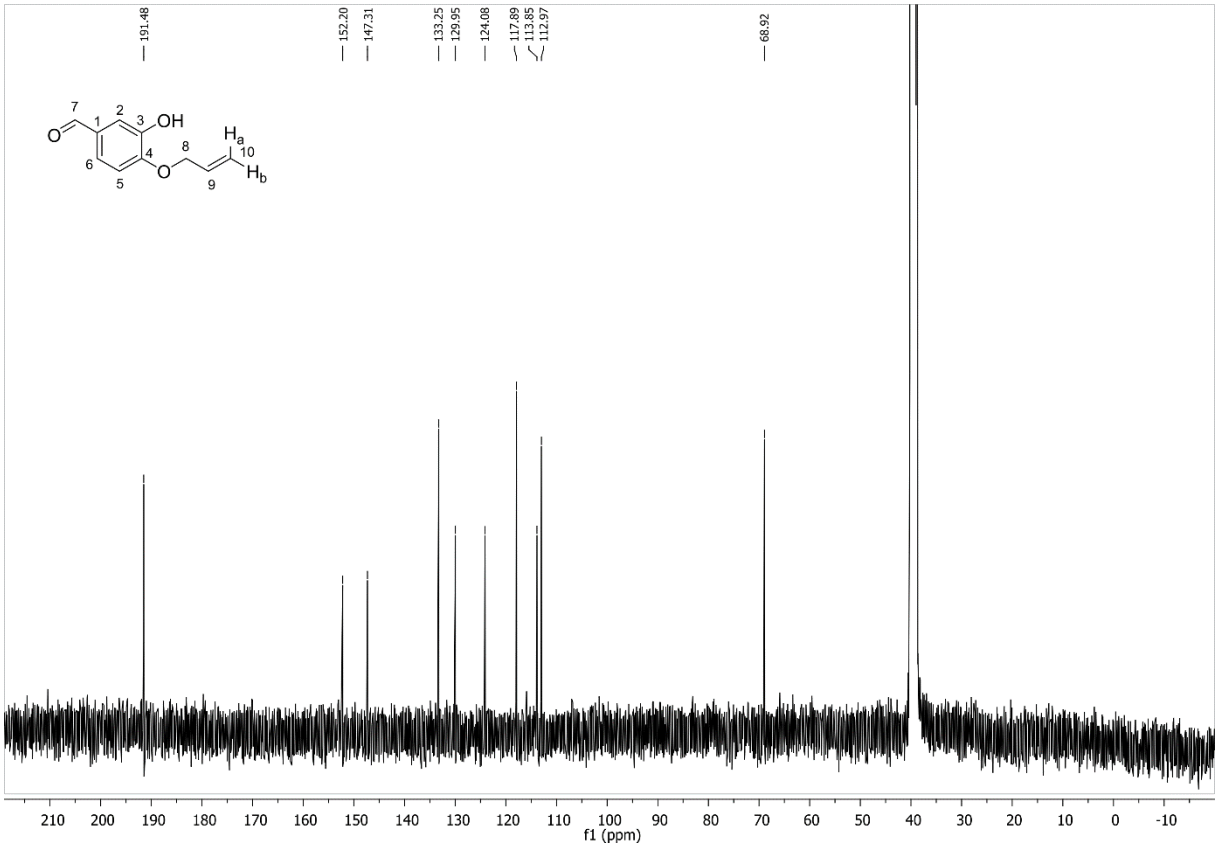

Figure S16. ^{13}C NMR spectrum of 4-allyloxy-3-hydroxybenzaldehyde (**8**).

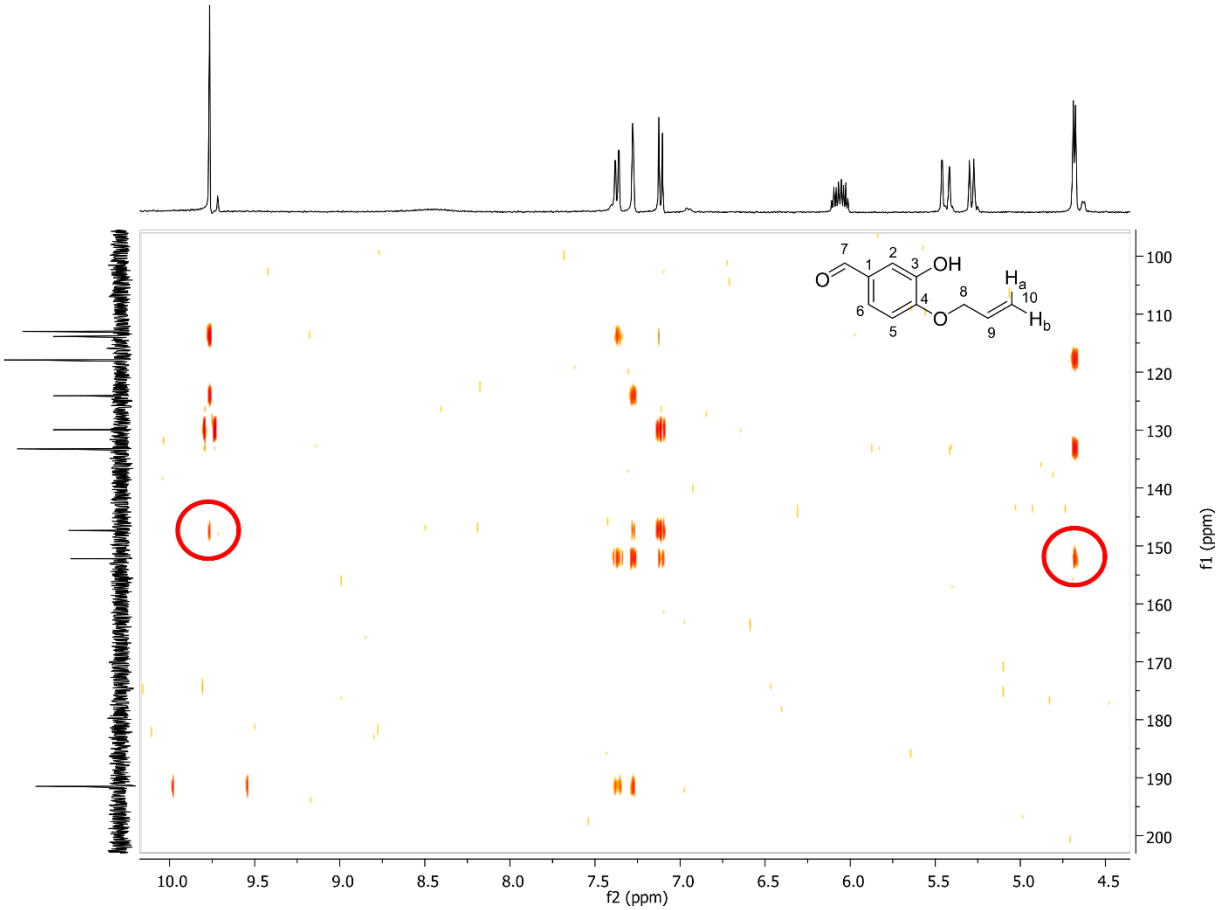

Figure S17. HMBC spectrum of 4-allyloxy-3-hydroxybenzaldehyde (**8**). Signals that define the regioisomer are highlighted.

***S*-propyl homocysteine (3).** ^{1}H NMR, H,H-COSY (400 MHz, D_2O): δ (ppm) =8.36 (s, 2H, 2-H, 8-H), 6,07 (d, J = 3.7 Hz, 1H, 1′-H), 4.82–4.70 (m, 1H, 2′-H), 4.51 (pseudo-t, J = 5.8 Hz, 1H, 3′-H), 4.48–4.39 (m, 1H, 4′-H), 3.99–3.89 (m, 1H, H_α), 3.88–3.79 (m, 2H, 5′-H), 3.62–3.38 (m, 2H, H_γ), 3.36–3.26 (m, 2H, 1″-H), 2.39–2.20 (m, 2H, H_β), 1.78–1.64 (m, 2H, 2″-H), 0.94–0.80 (m, 3H, 3″-H); ^{13}C NMR, DEPT-135, HSQC, HMBC (101 MHz, D_2O): δ (ppm) = 170.7 (COOH), 150.0 (6), 148.0 (4), 144.6 (2), 143.6 + 143.5 (8), 119.3 (5), 90.0 (1′), 78.6 + 78.5 (4′), 73.1 + 73.0 (2′), 72.8 (3′), 51.5 (5′), 42.7 + 42.0 (1″), 41.7 (α), 36.3 +36.2 (γ), 25.1 + 25.0 (β), 17.5 + 17.3 (2″), 11.9 (3″).

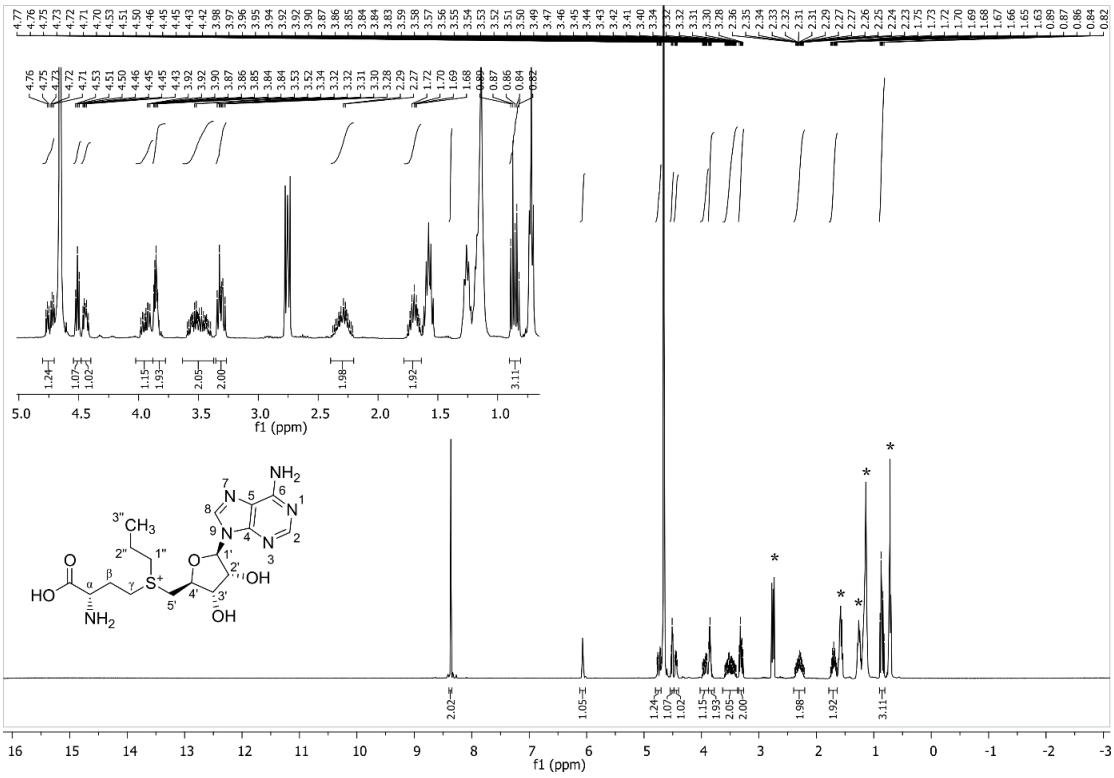

Figure S18. ^{1}H NMR spectrum of SAP (**3**) in the form of heptane sulfonate salt. Signals derived from heptane sulfonate are assigned asterisks.

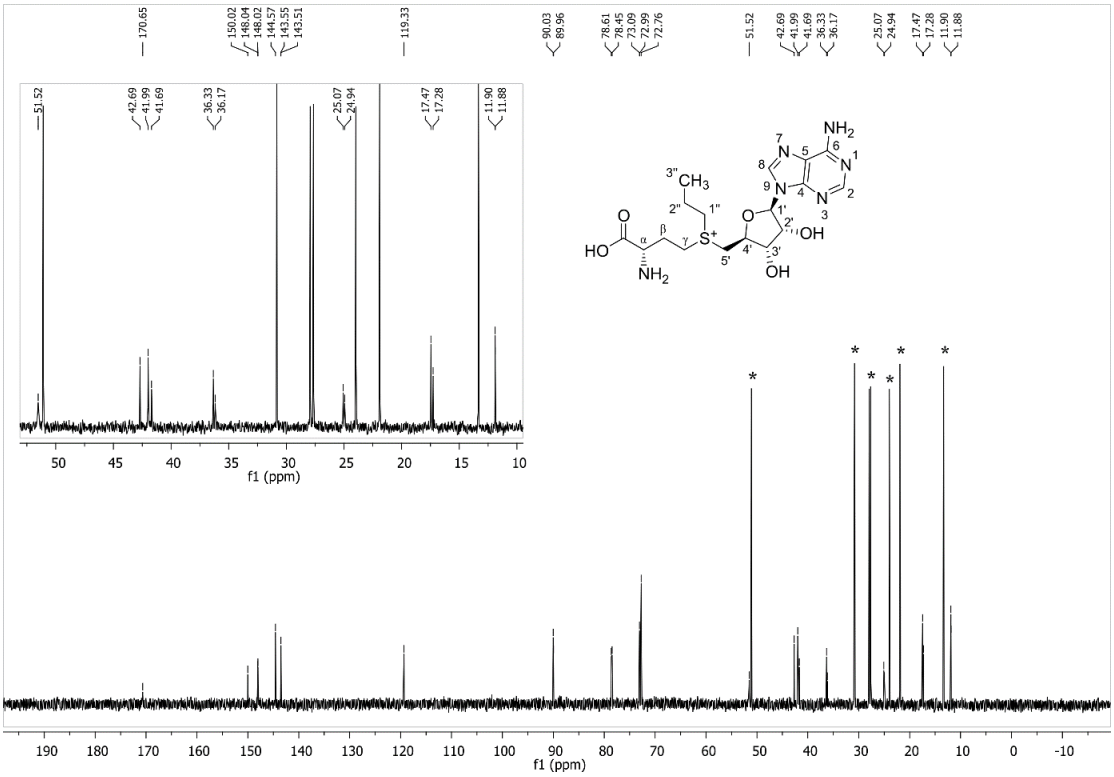

Figure S19. ^{13}C NMR spectrum of SAP (**3**) in the form of heptane sulfonate salt. Signals derived from heptane sulfonate are assigned asterisks.

Experimental procedures

Materials

Chemical reagents were purchased from Sigma Aldrich (Darmstadt, Germany), Alfa Aesar (Kandel, Germany), Fluorochem (Hadfield, UK), and Merck (Darmstadt, Germany), and were at least 95% pure. Reagents and solvents used for HPLC were purchased from Carl Roth GmbH (Karlsruhe, Germany) and VWR (Darmstadt, Germany), and were of HPLC grade. Molecular biology enzymes and kits were purchased from New England Biolabs (Ipswich, MA, US) unless otherwise stated. Oligonucleotides were purchased from Thermo Fisher Scientific (Hennigsdorf, Germany).

Method S1 Genes, protein expression, and mutagenesis

Method S1.1 Expression vectors

DNA sequences encoding the soluble form of *Homo sapiens* catechol *O*-methyltransferase (COMT) and the halide methyltransferases from *Arabidopsis thaliana* (*At*HMT), *Chloracidobacterium thermophilum* (*Ct*HMT), and *Raphanus sativus* (*Rs*HMT) were codon-optimized for expression in *Escherichia coli*. Genes were synthesized and cloned into pET-28a(+) or pET-28b(+) by BioCat GmbH (Heidelberg, Germany). The resulting constructs encoded either N- or C-terminal His_6-tags (amino acid sequences for all proteins are given in the section *Protein sequences*). The empty pET-28a(+) vector (Novagen®) was purchased from Merck (Darmstadt, Germany). The C-terminally His_6-tagged T133M-Y326L mutant of *Clarkia breweri* isoeugenol *O*-methyltransferase (IeOMT) in pET-21b(+) was described in our previous work.[2] All HMTs and MTs, as well as the empty pET-28a vector, were transformed into chemically competent *E. coli* BL21 Δmtn (DE3) cells (Method S1.3) using a standard heat-shock protocol.

Method S1.2 Site-saturation mutagenesis

Saturation mutagenesis was performed using mutagenesis PCR. Degenerate (NNK) oligonucleotides (Table S6) and the wild-type *At*HMT-encoding plasmid (DNA sequence is given below Table S6) were used. PCRs contained 1 x *Pfu* buffer, 2% DMSO, 200 nM each of forward and reverse primers, dNTPs (250 µM each), 0.2 ng/µl of template DNA (pET-28a-*At*HMT), and 0.05 U/µl of *Pfu* polymerase (Roboklon GmbH, Berlin, Germany). After initial denaturation for 1 min at 95 °C, 18 cycles of denaturation at 95 °C for 30 s, annealing at

60 °C for 1 min, and extension at 68 °C for 6.5 min were performed, followed by a final extension at 68 °C for 13 min. PCR products were treated twice by DpnI digestion to ensure complete removal of the template DNA.[3] The DpnI-digested PCR mixtures (5 µl) were used for heat shock transformation of chemically competent *E. coli* BL21 Δmtn (DE3) cells. Transformations were plated on LB Miller agar containing 50 µg/ml kanamycin and incubated overnight at 37 °C.

Table S6. Sequences of the degenerate (NNK) oligonucleotides used for site-saturation mutagenesis.

Primer	Sequence (5′-3′)
P20 NNK forward	ggcggtaatgtgattccgacc**nnk**gaagaagttgcaacctttctg
P20 NNK reverse	cagaaaggttgcaacttcttc**mnn**ggtcggaatcacattaccgcc
V23 NNK forward	atgtgattccgaccccggaagaa**nnk**gcaacctttctgcataaaac
V23 NNK reverse	gttttatgcagaaaggttgc**mnn**ttcttccggggtcggaatcacat
L27 NNK forward	cccggaagaagttgcaacctt**nnk**cataaaaccgttgaagaaggcg
L27 NNK reverse	cgccttcttcaacggttttatg**mnn**aaaggttgcaacttcttccggg
W36 NNK forward	gcataaaaccgttgaagaaggcggt**nnk**gaaaaatgctgggaagaagaaatta
W36 NNK reverse	taatttcttcttcccagcatttttc**mnn**accgccttcttcaacggttttatgc
W47 NNK forward	ggaagaagaaattaccccg**nnk**gatcagggtcgtgcaaccc
W47 NNK reverse	gggttgcacgaccctgatc**mnn**cggggtaatttcttcttcc
Y139 NNK forward	gtccgaccgaactgtttgatctgatttttgat**nnk**gtgttcttctgtgcaat
Y139 NNK reverse	attgcacagaagaacac**mnn**atcaaaaatcagatcaaacagttcggtcggac
V140 NNK forward	cgtccgaccgaactgtttgatctgatttttgattat**nnk**ttcttctgtgcaatcgaac
V140 NNK reverse	gttcgattgcacagaagaa**mnn**ataatcaaaaatcagatcaaacagttcggtcggacg
C143 NNK forward	ctgatttttgattatgtgttcttc**nnk**gcaatcgaaccggaaatgcgccc
C143 NNK reverse	gggcgcatttccggttcgattgc**mnn**gaagaacacataatcaaaaatcag
Y172 NNK forward	ggcgaactgattaccctgatg**nnk**ccgattaccgatcatgttggt
Y172 NNK reverse	accaacatgatcggtaatcgg**mnn**catcagggtaatcagttcgcc
R214 NNK forward	aatccgcatgccattccgacc**nnk**aaaggtaaagaaaaactgggc
R214 NNK reverse	gcccagttttctttacctttt**mnn**ggtcggaatggcatgcggatt

DNA sequence of the wild-type *At*HMT template used for mutagenesis

ATGGGCAGTAGTCATCATCATCATCACCATAGTAGTGGTCTGGTGCCGCGCGGCAGTCATATGGCCGAAGAACAGCAGAATAGTGA
TCAGAGTAATGGCGGTAATGTGATTCCGACCCCGGAAGAAGTTGCAACCTTTCTGCATAAAACCGTTGAAGAAGGCGGTTGGGAAA
AATGCTGGGAAGAAGAAATTACCCCGTGGGATCAGGGTCGTGCAACCCCGCTGATTGTGCATCTGGTGGATACCAGCAGCCTGCCG
CTGGGTCGCGCCTTAGTGCCGGGTTGCGGTGGTGGTCATGATGTGGTTGCCATGGCCAGTCCGGAACGCTTTGTTGTTGGTCTGGA
TATTAGTGAAAGCGCCCTGGCAAAAGCCAATGAAACCTATGGTAGCAGTCCGAAAGCAGAATATTTTAGCTTTGTTAAAGAGGATG
TGTTCACCTGGCGTCCGACCGAACTGTTTGATCTGATTTTTGATTATGTGTTCTTCTGTGCAATCGAACCGGAAATGCGCCCGGCA
TGGGCAAAAAGTATGTATGAACTGCTGAAACCGGATGGCGAACTGATTACCCTGATGTATCCGATTACCGATCATGTTGGTGGCCC
GCCGTATAAAGTTGATGTTAGCACCTTTGAAGAAGTGCTGGTGCCGATTGGCTTTAAAGCCGTGAGCGTGGAAGAAAATCCGCATG
CCATTCCGACCCGTAAAGGTAAAGAAAAACTGGGCCGCTGGAAAAAGATTAATTAA

Method S1.3 Construction of the MTA/SAH nucleosidase knockout *E. coli* BL21(DE3) strain

As reported by Liao and Seebeck, the 5′-methylthioadenosine/*S*-adenosyl homocysteine (MTA/SAH) nucleosidase from *E. coli* BL21(DE3) can degrade the substrate SAH to adenine and the enzyme cannot be completely removed by immobilized metal-affinity chromatography and size exclusion chromatography.[1] Thus, an MTA/SAH nucleosidase knockout strain of *E. coli* BL21(DE3), named *E. coli* BL21 Δmtn (DE3), was constructed for the expression of HMTs and MTs. The *E. coli* BL21 Δmtn (DE3) strain was constructed using a previously developed two-plasmid-based CRISPR-Cas9 system.[4] The two key plasmids pCas and pTargetF (plasmid IDs #62225 and #62226) were purchased from Addgene (Watertown, MA, US). The pTarget-dmtn plasmid was first constructed by engineering the flanking sequence of the *mtn* gene by assembly of three DNA fragments, the mtn-Up fragment and the mtn-Down fragment, amplified from the *E. coli* genome using the corresponding primers (Table S7), and the pTarget fragment amplified from the pTargetF plasmid using the corresponding primers (Table S7). The three fragments were assembled using the SLiCE cloning method.[5] Next, the gRNA was introduced with the dmtn-gRNA primers using the Q5 Site-Directed Mutagenesis Kit from New England Biolabs. The resulting pTarget-dmtn plasmid was sequenced to confirm introduction of the gRNA and the flanking sequence of the *mtn* gene. The *E. coli* BL21 Δmtn (DE3) strain was constructed by using pCas and pTarget-dmtn according to a previously developed procedure,[4] briefly outlined here. 1) Transform the pCas plasmid into chemically competent *E. coli* BL21(DE3) cells following a standard heat-shock protocol. 2) Prepare electrocompetent cells of *E. coli* BL21(DE3) pCas with the arabinose-inducible λ-Red system. 3) Introduce the pTarget-dmtn plasmid by electroporation. 4) Select on LB agar plates containing 50 μg/ml kanamycin (for pCas) and 50 μg/ml streptomycin (for pTarget-dmtn). 5) Perform colony PCR for genotyping the colonies. 6) Sequentially cure the plasmid pTarget-dmtn (by adding 1 mM IPTG) and pCas (by culturing at 37°C for 12 h). The resulting *E. coli* BL21 Δmtn (DE3) strain was confirmed by PCR amplification and sequencing the genomic DNA flanking the *mtn* gene. Chemically competent *E. coli* BL21 Δmtn (DE3) cells were prepared using the Hanahan method.[6]

Table S7. Oligonucleotides used for construction of the MTA/SAH nucleosidase knockout strain *E. coli* BL21 Δmtn (DE3).

Primer	Sequence (5′-3′)
mtn-Up-forward	gagtcgacctgcagaagcttgaaaccagtcatttatcgctgc
mtn-Up-reverse	cagtgacttaagatttactcgcgataagccc
mtn-Down-forward	gagtaaatcttaagtcactgttcagggcgct
mtn-Down-reverse	gagctgcacatgaactcgaggcggattaatgccgaattgcag
pTarget-forward	ctcgagttcatgtgcagctc
pTarget-reverse	aagcttctgcaggtcgactc
dmtn-gRNA-forward	tctgttggtcgttttagagctagaaatagcaagtt
dmtn-gRNA-reverse	accgttgatgactagtattatacctaggactgagc

Method S2 High-throughput screening

Method S2.1 Expression of variants in the NNK libraries

For each NNK library, 96 colonies were picked into 96-well microtiter plates filled with 150 µl of lysogeny broth (LB) containing 50 µg/ml kanamycin and grown overnight at 37°C, shaking at 700 rpm in an MTP shaker (Edmund Bühler GmbH, Bodelshausen, Germany). Terrific Broth (1 ml in 96-deepwell plates) containing 50 µg/ml kanamycin and 100 µM of isopropyl β-D-1-thiogalactopyranoside (IPTG) were inoculated with 50 µl of the pre-cultures and incubated at 30°C (900 rpm) for 24 h. The remaining pre-cultures were mixed with glycerol to a final concentration of 40% (v/v) and stored at -80 °C. The cells grown in deep-well plates were collected by centrifugation at 4,000 *g* for 20 min (4 °C). Cell pellets were resuspended in 250 µl of lysis buffer (1 mg/ml lysozyme, 10 µg/ml DNase, and 0.1 × BugBuster ® Protein Extraction Reagent (Novagen®) in 50 mM sodium phosphate (pH 7.5) by shaking at 700 rpm (30°C) for 2 h. Cell debris was removed by centrifugation at 4,000 *g* for 20 min (4°C) and the resulting supernatant was used for HMT assays.

Method S2.2 HMT assay and general screening workflow

Libraries were screened in 96-well microtiter plates. Reactions contained 1 mM SAH (1 µl of a 100 mM stock in DMSO), 5 mM ethyl iodide (5 µl of a 100 mM stock in DMSO) and 94 µl of crude cell lysate, for a final assay volume of 100 µl, and were incubated at room temperature for 30 min. Ethyl iodide stocks in DMSO were freshly prepared for each experiment to avoid hydrolysis. After the 30 min incubation, 1 µl of each reaction mixture was added to 50 µl of iodide assay reagent (Method S3.2) in transparent 96-well polystyrene microtiter plates. The plates were shaken immediately and then incubated at room temperature for 30 min. The production of iodide by the HMT reaction was detected by observing the color of the assay solution (Figures S2 and S4). Hits showing higher activities than the wild-type *At*HMT were cultivated from the respective glycerol stocks. Plasmid DNA was isolated (innuPREP Plasmid Mini Kit 2.0, Analytic Jena, Jena, Germany) and sent for Sanger sequencing (Eurofins Genomics Germany GmbH, Ebersberg, Germany).

Method S3 The iodide assay for high-throughput screening

Method S3.1 Assay principle

We developed a sensitive and convenient iodide assay based on our published HOX assay for halides.[7] The assay described here has the advantage of being very sensitive to iodide but relatively insensitive to chloride, making it ideal for screening using chloride-containing crude lysates. Iodide was first converted to hypoiodous acid (HOI) by a vanadium-dependent chloroperoxidase from *Curvularia inaequalis* (*Ci*VCPO, Method S3.4). The *Ci*VCPO uses hydrogen peroxide to oxidize iodide to HOI under mild conditions. The bleach HOI is detected by oxidation of the chromogen 3,3′,5,5′-tetramethylbenzidine (TMB).[8] TMB is first converted to the one-electron oxidized cation radical which is in equilibrium with the TMB-diimine complex (blue, λ_{max} = 570 nm) and finally to the two-electron oxidized diimine product (orange, λ_{max} = 460 nm) (Figure S2a).[8a] In the assay setup we used, iodide concentrations from 5 µM to 10 mM could be detected. For lower concentrations, the assay turns blue and for higher concentrations the mixture turns purple, copper, or orange (Figure S2b) and the maximum absorption shifts from 570 to 460 nm (Figure S2c). We used only 1 µl of sample in a 50 µl iodide assay so much less than 5 µM of iodide could be detected by adjusting the sample volume. Importantly, the iodide assay is not sensitive to millimolar concentrations of chloride (Figure S2b).

Method S3.2 Preparation of the assay reagent

An assay solution containing 1.37 U/ml *Ci*VCPO, 25 mM TMB, 2 mM hydrogen peroxide, and 1 mM sodium orthovanadate in 20 mM phosphate (pH 6.0) was used for preliminary experiments. However, to simplify the assay setup for high-throughput screening, we used a commercially available premixed solution of TMB and H_2O_2 in a mildly acidic buffer (Liquid Substrate System for Membranes; Sigma Aldrich; Catalog Number T0565). The concentrations of the individual components in this proprietary mixture are unknown but the commercial solution was suitable for our purposes. We prepared our iodide assay reagent by adding recombinantly expressed *Ci*VCPO, to a final concentration of 1.37 U/ml, to the Liquid Substrate System. Expression and purification of the *Ci*VCPO is described in Method S3.4.

Method S3.3 Iodide quantification and calibration curves

For the quantification of iodide, the iodide assay was carried out in transparent 384-well polystyrene microtiter plates at room temperature. Absorbance measurements were performed using a Tecan Infinite M200PRO3 Plate Reader (Tecan, Männedorf, Switzerland). Samples or standards (1 µl) were added to iodide assay reagent (50 µl) and the initial rate of change in absorbance at 570 nm determined. The calibration curve for iodide was determined using potassium iodide (KI) solutions ranging from 5 µM to 400 µM. All reactions were performed in triplicate. The rate of change in absorbance at 570 nm (v (A_{570nm}/s)) showed a linear relationship to iodide concentration from 5 µM to 400 µM (Figure S3a).

Method S3.4 Expression, purification, and activity determination of *Ci*VCPO

The *Ci*VCPO was expressed from the pBAD-VCPO plasmid in *E. coli* TOP10 as previously described.[7] In short, a culture of 10 ml of LB medium containing 100 µg/ml ampicillin was inoculated with a single colony from an LB agar plate containing 100 µg/ml ampicillin and incubated overnight at 37°C. The overnight culture was used to inoculate a 1 L culture of LB medium containing 100 µg/ml ampicillin. The culture was incubated at 37°C (180 rpm) until OD_{600} reached ~0.5. Expression was then induced by the addition of 0.02% L-arabinose, followed by incubation at 25°C for 24 h. Cells were harvested by centrifugation at 4500 *g* for 30 min (4°C) and resuspended in ice-cold lysis buffer (1 ml per gram of cells). The lysis buffer was composed of 50 mM Tris-H_2SO_4 (pH 8.1) containing 2 mg/ml lysozyme, 1 mg/ml DNaseI, and cOmplete™ protease inhibitor cocktail (Roche, Mannheim, Germany). The resuspended cells were lysed by sonication on ice (three cycles of 5 min; 50% pulse and 50% power) using a SONOPULS HD 2070 (BANDELIN electronic GmbH & Co. KG, Berlin, Germany). The crude

lysate was clarified at 4 °C by centrifugation at 10,000 *g* for 1 h. The clarified lysate was transferred to a new tube, thoroughly mixed with an equal volume of isopropanol, and incubated on ice for 20 min. Precipitated proteins were removed by centrifugation at 10,000 *g* for 30 min (4°C). The *Ci*VCPO was then purified by chromatography on a 5 ml DEAE Sephacel column equilibrated with 50 mM Tris-H_2SO_4 (pH 8.1). The column was washed with 25 ml of 50 mM Tris-H_2SO_4 (pH 8.1) and then with 25 ml of the same buffer containing 100 mM sodium chloride. Protein was eluted from the column using 50 mM Tris-H_2SO_4 (pH 8.1) containing 1 M sodium chloride. The eluate (30 ml) was dialyzed three times (twice for 4 h and then overnight) against 4.5 L of 50 mM sodium phosphate (pH 8.0) supplemented with 100 µM sodium orthovanadate. The orthovanadate converts the apoenzyme to the active vanadium-bound holoenzyme. Protein concentration was determined by measuring absorbance at 280 nm using a NanoDrop™ (Thermo Fisher, Hennigsdorf, Germany). The specific activity of *Ci*VCPO was determined using the monochlorodimedone assay. Bromination of monochlorodimedone results in a decrease in absorbance at 290 nm ($\Delta\varepsilon$ = 20,000 $M^{-1}cm^{-1}$). Reactions (600 µl) containing 42 µM monochlorodimedone, 100 µM bromide, 8.8 mM H_2O_2, and 1 mM orthovanadate in 20 mM phosphate (pH 6.0) were initiated by addition of 10 µl (4.5 µg) of purified *Ci*VCPO. The decrease in absorbance at 290 nm was monitored using a 1 cm-pathlength quartz cuvette and a JASCO V-550 spectrophotometer (JASCO, Easton, MD, US). Specific activity was expressed as µmol monochlorodimedone brominated/min/(mg *Ci*VCPO).

Method S4 Characterization of purified HMTs

Method S4.1 Expression and purification of HMTs and MTs

All HMTs and MTs were transformed into chemically competent *E. coli* BL21 Δmtn (DE3) cells for protein expression. Pre-cultures (5 ml LB medium containing 50 µg/ml kanamycin for pET-28 plasmids or 100 µg/ml ampicillin for pET-21 plasmids) were inoculated with single colonies and incubated overnight at 37°C. For the *At*HMT mutants, pre-cultures were inoculated from glycerol stocks of the NNK libraries (2% (v/v)). The cells were grown in Terrific Broth (TB) containing antibiotics (50 µg/ml kanamycin for pET-28 plasmids or 100 µg/ml ampicillin for pET-21 plasmids) at 37°C for about 2 h until OD_{600} reached ~0.7. Cultures were then cooled to 20°C before IPTG was added to a final concentration of 200 µM. Cultures were then incubated at 20°C for another 20 h. Cells were harvested by centrifugation at 10,000 *g* at 4°C for 10 min. Cell pellets were resuspended in lysis buffer (20 mM sodium phosphate, 500 mM sodium chloride, and 20 mM imidazole, pH 7.5) and lysed by sonication on ice (as described in Method S3.4). Lysates were clarified by centrifugation at 10,000 *g* and 4°C for 1 h. The His_6-tagged recombinant proteins were purified by immobilized metal-affinity chromatography as follows. The clarified lysates were loaded onto 2 ml of Roti®garose-His/Co Beads (Carl Roth, Karlsruhe,

Germany) equilibrated with lysis buffer. After incubation on ice for 15 min, the flow-through was discarded and weakly bound proteins were removed by washing the resin with lysis buffer. The target proteins were then eluted with elution buffer (20 mM sodium phosphate, 500 mM sodium chloride, and 200 mM imidazole, pH 7.5) and desalted using PD-10 desalting columns (GE healthcare, Amersham, UK) equilibrated with storage buffer. Storage buffer was chloride-free 50 mM sodium phosphate (pH 7.5) prepared by dissolving 0.041 mol Na_2HPO_4 and 0.0094 mol NaH_2PO_4 in 1 L of Milli-Q water. Further desalting was achieved by dilution into 40 volumes of storage buffer and concentration using 10 kDa MWCO Vivaspin™ protein concentrators (Sartorius AG, Germany, Göttingen). Protein concentrations were determined by measuring absorbance at 280 nm using a NanoDrop™ (Thermo Fisher, Hennigsdorf, Germany). Extinction coefficients (280 nm) for all proteins are given in the section *Protein sequences*. Protein purities were analyzed by SDS-PAGE.[9]

Method S4.2 HMT specific activity and kinetic measurements

HMTs and mutants were assayed using various haloalkanes. Reaction mixtures (50 µl) contained 1 mM SAH, 10 mM haloalkane, and the purified enzyme in 50 mM chloride-free sodium phosphate (pH 7.5). Reactions were incubated in an Eppendorf Thermomixer at 25°C and 1000 rpm. All haloalkane stocks in DMSO were freshly prepared before the reaction to avoid hydrolysis. Purified enzymes were added to a final concentration of 0.15 mg/ml (5.46 µM wild-type or mutant *At*HMT) for methyl iodide assays. For other iodoalkanes, 2 mg/ml protein (72.85 µM wild-type or mutant *At*HMT) was used. The reaction time was 10 min for methyl and ethyl iodide and 4 h (Table S1) or 16 h (Figure S7) for all other iodoalkanes. After incubation, 1 µl of reaction mixture was added to 50 µl iodide assay reagent and the iodide concentration determined as described in Method S3.3. Kinetic measurements were carried out at various concentrations of alkyl iodide while keeping the SAH concentration constant at 1 mM. Initial velocities (amount of iodide produced per minute) were fit to the Michaelis-Menten model using GraphPad Prism 6.0 (GraphPad Software Inc., San Diego, CA, US) to determine the k_{cat} and K_m values. All reactions were measured in triplicate. Rates of HMT-dependent iodide formation were corrected for autohydrolysis, which was determined for each iodoalkane at each concentration employed.

Method S4.3 HPLC analysis of MT and HMT reactions

Reactions using the purified HMTs were performed as described for the iodide assay (Method S2.2) and quenched by adding an equal volume of acetonitrile. Samples were vortexed vigorously and then centrifuged at 17,000 *g* for 10 min to remove precipitated protein.

The supernatants were transferred to HPLC sample vial inserts prior to HPLC analysis. Analyses were performed on a Hitachi Elite LaChrom system equipped with a Kinetex EVO C18 (4.6 x 250 mm column, 5 µm particle size) reversed-phase column (Phenomenex, Torrance, CA, US). For separation of SAH, SAM, and SAM analogues, the mobile phases were (A) 10 mM sodium phosphate containing 5 mM sodium 1-heptanesulfonate (pH 3.5), and (B) acetonitrile. A gradient from 5% to 20% (B) over 10 min was followed by a gradient from 20% to 5% B over 1 min, then kept constant for 4 min. The flow rate was constant at 1 ml/min. SAH, SAM, and SAM analogues were detected at 260 nm and quantified using a SAM (J&K Chemical Ltd., China, Beijing) standard and calibration curve (Figure S3b).[10] Previously reported methods were adapted for separations of luteolin (**5**) and its ethylated product (**6**), and 3,4-dihydroxybenzaldehyde (**7**) and its propylated or allylated (**8**) products.[2, 11] A Kinetex EVO C18 (4.6 x 250 mm column, 5 µm particle size) reversed-phase column was used. The mobile phases were 0.1% acetic acid (A) and acetonitrile (B). A gradient elution from 20% to 60% (B) over 5 min, was followed by a gradient from 60% to 20% (B) over 1 min, and then kept constant for 4 min.

Method S5 Preparative-scale HMT reactions

Method S5.1 Preparative-scale production of SAM analogues and alkylated compounds

Scaled-up production of ethylated luteolin (**6**), and propylated or allylated DHBA (**8**) was performed as described in Table S5. In short, 10 or 20 mg of the MT substrate, 80 mM alkyl iodide, 100 µM SAH, MT, and HMT were shaken (1200 rpm) in HPLC vials at 25°C. Subsequently, the reaction mixtures were extracted three times with an equal volume of ethyl acetate. Ethyl acetate was then removed by rotary evaporation and the residues dissolved in hexadeuterodimethyl sulfoxide (DMSO-d_6) for NMR spectroscopy. The alkylated products were analyzed by HPLC (Method S4.3) and then purified by preparative HPLC (Method S5.2).

Preparative-scale production of SAE, SAP, and SAA started with 15 mg SAH (10 mM), 80 mM of the corresponding alkyl iodide, and purified V140T-*At*HMT (Table S4). Reactions (3.9 ml of each) were performed in HPLC vials at 25°C, with shaking at 1200 rpm, for 14 to 24 h. Subsequently, the reaction mixtures were extracted three times with an equal volume of diethyl ether to remove the remaining alkyl iodides and to precipitate protein. The supernatants containing the SAM analogues were analyzed by analytical HPLC (Method S4.3) and then purified by preparative HPLC (Method S5.2).

Method S5.2 Preparative HPLC purification

Prior to purification, SAM analogues and alkylated compounds were analyzed using an analytical LiChrospher® 100 RP-18 (5 µm) LiChroCART® (250×4 mm, Merck) column. The preparative column was a LiChrospher® 100 RP-18 (5 µm) Hibar® RT (250×25 mm, Merck). Both HPLCs were equipped with Shimadzu devices CBM-20A, LC-20A P, SIL-20A, FRC-10A, and an SPD 20A UV/Vis detector. The mobile phases and gradient elution methods were the same as for measurements on the Kinetex EVO C18 column (Method S4.3) and the flow rate was 32 ml/min. Product fractions were collected and dried using a rotary evaporator, lyophilized, and dissolved in DMSO-d_6 (for **6** and **8**) or D_2O (for **3**) for NMR spectroscopy (Method S5.3).

Method S5.3 NMR spectroscopy

NMR spectra were recorded on a Bruker Avance III instrument (^{1}H NMR: 400 MHz, ^{13}C NMR: 100.6 MHz). Chemical shifts were referenced to tetramethylsilane (TMS) as internal standard in DMSO-d_6 and reported in parts per million (ppm). For D_2O as solvent, chemical shifts were referenced to residual H_2O in the samples. Signals are described using the abbreviations: br = broad, s = singlet, d = duplet, t = triplet, q = quartet, m = multiplet, and combinations thereof.

Protein sequences

Molecular weights and extinction coefficients, used for quantification of protein concentration by measurements of absorbance at 280 nm, were calculated using the ExPASy ProtParam tool.

Arabidopsis thaliana halide methyltransferase

- NCBI Reference Sequence: NP_001318420.1
- Extinction coefficient (280 nm): 42065 $M^{-1}cm^{-1}$
- Molecular weight: 27.452 kDa

MGSSHHHHHHSSGLVPRGSHMAEEQQNSDQSNGGNVIPTPEEVATFLHKTVEEGGWEKCWEEEITPWDQ
GRATPLIVHLVDTSSLPLGRALVPGCGGGHDVVAMASPERFVVGLDISESALAKANETYGSSPKAEYFS
FVKEDVFTWRPTELFDLIFDYVFFCAIEPEMRPAWAKSMYELLKPDGELITLMYPITDHVGGPPYKVDV
STFEEVLVPIGFKAVSVEENPHAIPTRKGKEKLGRWKKIN

Chloracidobacterium thermophilum halide methyltransferase

- GenBank: AEP12557.1
- Extinction coefficient (280 nm): 65680 $M^{-1}cm^{-1}$
- Molecular weight: 24.617 kDa

MGHHHHHHAENLYFQGSGLGMDADTASFWEEKYRADLTAWDRGGVSPALEHWLAEGALKPGRILIPGCG
YGHEVLALARRGFEVWGLDIALTPVRRLQEKLAQAGLTAHVVEGDVRTWQPEQPFDAVYEQTCLCALSP
EDWPRYEAQLCRWLRPGGRLFALWMQTDRPGGPPYHCGLEAMRVLFALERWRWVEPPQRTVPHPTGFFE
YAAILERLV

Raphanus sativus halide methyltransferase

- GenBank: BAH84870.1
- Extinction coefficient (280 nm): 46535 $M^{-1}cm^{-1}$
- Molecular weight: 26.530 kDa

MAEGQQNSGNSNGENIIPPEDVAKFLPKTVEEGGWEKCWEDGVTPWDQGRATPLVVHLVESSSLPLGRA
LVPGCGGGHDVVAMASPERYVVGLDISESALEKAAETYASSPKAKYFTFVKEDFFTWRPSELFDLIFDY
VVFCAIEPEMRAAWAKTMYELLKPDGELITLMYPITDHDGGPPYKVAVSTYEDVLVPVGFKAVSIEENP
YSIATRKGKEKLGRWKKINKLAAALEHHHHHH

Homo sapiens catechol *O*-methyltransferase (soluble-form)

- NCBI Reference Sequence: NP_009294.1
- Extinction coefficient (280 nm): 23295 $M^{-1}cm^{-1}$
- Molecular weight: 24.449 kDa

MGDTKEQRILNHVLQHAEPGNAQSVLEAIDTYCEQKEWAMNVGDKKGKIVDAVIQEHQPSVLLELGAYC
GYSAVRMARLLSPGARLITIEINPDCAAITQRMVDFAGVKDKVTLVVGASQDIIPQLKKKYDVDTLDMV
FLDHWKDRYLPDTLLLEECGLLRKGTVLLADNVICPGAPDFLAHVRGSSCFECTHYQSFLEYREVVDGL
EKAIYKGPGSEAGPGSSGHHHHHH

Curvularia inaequalis vanadium-dependent chloroperoxidase

- Described by Hasan et al.[12]
- Extinction coefficient (280 nm): 93280 $M^{-1}cm^{-1}$
- Molecular weight: 70.105 kDa

MKKLLFAIPLVVPFYSHSTMASHMGSVTPIPLPKIDEPEEYNTNYILFWNHVGLELNRVTHTVGGPLTG
PPLSARALGMLHLAIHDAYFSICPPTDFTTFLSPDTENAAYRLPSPNGANDARQAVAGAALKMLSSLYM
KPVEQPNPNPGANISDNAYAQLGLVLDRSVLEAPGGVDRESASFMFGEDVADVFFALLNDPRGASQEGY
HPTPGRYKFDDEPTHPVVLIPVDPNNPNGPKMPFRQYHAPFYGKTTKRFATQSEHFVADPPGLRSNADE
TAEYDDAVRVAIAMGGAQALNSTKRSPWQTAQGLYWAYDGSNLIGTPPRFYNQIVRRIAVTYKKEEDLA
NSEVNNADFARLFALVDVACADAGIFSWKEKWEFEFWRPLSGVRDDGRPDHGDPFWLTLGAPATNTNDI
PFKDPFPAYPSGHATFGGAVFQMVRRYYNGRVGTWKDDEPDNIAIDMMISEELNGVNRDLRQPYDPTAP
IEDQPGIVRTRIVRHFDSAWELMFENAISRIFLGVHWRFDAAAARDILIPTTTKDVYAVDNNGATVFQN
VEDIRYTTRGTREDPEGLFPIGGVPLGIEIADEIFNNGLKPTPPEIQPMPQETPVQKPVGQQPVKGMWE
EEQAPVVKEAP

References

[1] C. Liao, F. P. Seebeck, *Nat. Catal.* **2019**, *2*, 696-701.

[2] Q. Tang, Y. M. Vianney, K. Weisz, C. W. Grathwol, A. Link, U. T. Bornscheuer, I. V. Pavlidis, *ChemCatChem* **2020**, *12*, 3721–3727.

[3] M. T. Reetz, J. D. Carballeira, *Nat. Protoc.* **2007**, *2*, 891.

[4] Y. Jiang, B. Chen, C. Duan, B. Sun, J. Yang, S. Yang, *Appl. Environ. Microbiol.* **2015**, *81*, 2506-2514.

[5] Y. Zhang, U. Werling, W. Edelmann, *Nucleic Acids Res.* **2012**, *40*, e55-e55.

[6] R. Green, E. J. Rogers, *Methods Enzymol.* **2013**, *529*, 329.

[7] A. S. Aslan-Üzel, A. Beier, D. Kovář, C. Cziegler, S. K. Padhi, E. D. Schuiten, M. Dörr, D. Böttcher, F. Hollmann, F. Rudroff, M. D. Mihovilovic, T. Buryška, J. Damborský, Z. Prokop, C. P. S. Badenhorst, U. T. Bornscheuer, *ChemCatChem* **2020**, *12*, 1-9.

[8] a) P. D. Josephy, T. Eling, R. P. Mason, *J. Biol. Chem.* **1982**, *257*, 3669-3675; b) P. M. Bozeman, D. B. Learn, E. L. Thomas, *J. Immunol. Methods* **1990**, *126*, 125-133.

[9] U. K. Laemmli, *Nature* **1970**, *227*, 680-685.

[10] B. J. Law, A.-W. Struck, M. R. Bennett, B. Wilkinson, J. Micklefield, *Chem. Sci.* **2015**, *6*, 2885-2892.

[11] Q. Tang, U. T. Bornscheuer, I. V. Pavlidis, *ChemCatChem* **2019**, *11*, 3227-3233.

[12] Z. Hasan, R. Renirie, R. Kerkman, H. J. Ruijssenaars, A. F. Hartog, R. Wever, *J. Biol. Chem.* **2006**, *281*, 9738-9744.